Received: 19 October 2020 | Revised: 30 July 2021 | Accepted: 22 August 2021

DOI: 10.1111/rsp3.12472

ORIGINAL ARTICLE

On the link between temperature and regional COVID-19 severity: Evidence from Italy

Vicente Rios[1] | Lisa Gianmoena[2]

[1]Department of Economics, University of Milan, Via Festa del Perdono, 7, Milano, 20122, Italy

[2]Department of Economics and Management, University of Pisa, Cosimo Ridolfi 10, Pisa, 56124, Italy

Correspondence
Vicente Rios, Department of Economics, University of Milan, Via Festa del Perdono, 7, 20122 Milano, Italy.
Email: vicente.rios@unimi.it

Funding information
Ministerio de Economía y Competitividad, Grant/Award Number: ECO2016-76681-R

Abstract

This study analyzes the link between temperature and COVID-19 incidence in a sample of Italian regions during the period that covers the first epidemic wave of 2020. To that end, Bayesian model averaging techniques are used to analyze the relevance of temperature together with a set of additional climatic, demographic, social, and health policy factors. The robustness of individual predictors is measured through posterior inclusion probabilities. The empirical analysis provides conclusive evidence on the role played by temperature given that it appears as one of the most relevant determinants reducing regional coronavirus disease 2019 (COVID-19) severity. The strong negative link observed in our baseline analysis is robust to the specification of priors, the scale of analysis, the correction of measurement errors in the data due to under-reporting, the time window considered, and the inclusion of spatial effects in the model. In a second step, we compute relative importance metrics that decompose the variability explained by the model. We find that cross-regional temperature differentials explain a large share of the observed variation on the number of infections.

KEYWORDS
Bayesian model averaging, COVID-19, infections, Italian regions, spatial econometrics, temperatures

1 | INTRODUCTION

The coronavirus disease 2019 (COVID-19) pandemic, produced by the severe acute respiratory syndrome coronavirus 2 (SARS-CoV-2) pathogen, is likely to have been the most disruptive global shock to our societal organization since World War II, threatening the health systems and the functioning of the economy (International Monetary Found, 2020; World Health Organization, 2020a). Given that the management of the COVID-19 crisis is of major importance from a policy perspective, this study aims to increase our understanding of the drivers of the geographical variation in COVID-19 contagions.

One of the research questions that has received much attention in the COVID-19-related literature is the possible link between climatic factors and COVID-19 infections. The relationship between viral disease transmission and climatic factors has been well documented in numerous infectious diseases (World Health Organization, 2005). Disease agents and their vectors have specific environments that are optimal for growth, survival, transport, or dissemination; and climatic factors like precipitation, temperature, humidity, air circulation, and solar radiation intensity ultimately define such an environment.

As regards SARS-CoV-2, which is assumed to be propagated via (i) small airborne micro-droplets (also commonly referred to as 'aerosols') (Morawska et al., 2020; Morawska & Cao, 2020; Van Doremalen et al., 2020), (ii) larger respiratory droplets (which fall close to where they are expired), and (iii) direct contact with contaminated surfaces (fomites) (World Health Organization, 2020b), there are reasons to believe that both temperature and other climatic factors may exert an impact on the course of the pandemic (Chan et al., 2011, 2020; Makinen et al., 2009). Specifically, temperature may affect not only the susceptibility conditions of the host and the physical properties of the virion envelope, including its stability, but also the efficiency of the different routes of viral transmission (Duan et al., 2003; Lowen & Steel, 2014).

Our literature review shows that at least 27 studies have investigated the link between temperature and COVID-19 regional severity differentials. Nonetheless, the empirical evidence on this relationship is mixed, as it virtually fits all possibilities and reaches diverging conclusions. While we recognize these studies represent substantial progress in understanding the link between climate and the spread of COVID-19, many of them face important methodological problems affecting the validity of their conclusions (see Shakil et al., 2020 a critical review).

A first issue in this literature is that it is common to find studies that did not control for other factors that may correlate with both temperature and the epidemic indicator, which may severely bias parameter estimates. Some exceptions are Lin et al. (2020), Cartení et al. (2020), Paez et al. (2020), and Perone (2020), who do not only consider environmental controls but also a variety of alternative social and demographic characteristics. This point is also relevant from a theoretical perspective given that epidemics, in their early stages, could be controlled by processes other than the environment and climate. Second, although many researchers present some variations or sensitivity checks with respect to a baseline specification, all of them ignored the model uncertainty surrounding the data generating process (DGP) underlying COVID-19 contagion differentials across their sample units. Since it is often not clear a priori which set of variables are part of the 'true' regression model, a naive approach that ignores specification and data uncertainty may result in biased estimates, overconfident (too narrow) standard errors, and misleading inference and predictions. A third issue with existing analysis on the drivers of regional COVID-19 disparities is that they fail to derive a rank or a 'hierarchy' of the various factors in terms of their importance, thus hampering the consensus on what policies could be implemented to increase resilience against the pandemic. Fourth, most of the literature has overlooked the fact that the percentage of cases detected varies considerably across regions and time, which suggests the presence of measurement errors in the data and important problems of comparability and sample homogeneity (Russell et al., 2020).

To solve such issues, this study contributes to the literature investigating the linkages between climate and COVID-19 contagions in the following aspects.

First, in our baseline analysis, we investigate the link between temperature and contagions considering model uncertainty by means of Bayesian model averaging (BMA) techniques (Steel, 2020) in a sample of 21 NUTS-2 level

Italian regions for the period ranging from February 24 to April 15 of 2020. By computing posterior inclusion probabilities, which is the standard Bayesian measure of variable importance, we derive a probabilistic ranking of the importance of 14 factors that capture regional differences in (i) *institutional/health factors* and variables related to the regional authorities' policy response to the epidemic, (ii) *demographic factors*, (iii) *climatic and environmental characteristics*, and (iv) variables that measure the *degree of social connectedness and mobility* of the population.

Second, to complement the BMA analysis, we calculate relative importance metrics for regression models (Gromping, 2007; Johnson & LeBreton, 2004). These metrics perform a decomposition of the R^2 of the regression model, enabling a detailed analysis of the relative contribution of each variable to the explained variability of regional contagion differentials. The main advantage of this approach is that it allows the importance of each factor to be entangled taking into account its multivariate interactions with the other factors. A key difference of relative importance metrics with respect standard tools like analysis of variance (ANOVA) is that, unlike ANOVA, relative importance metrics employed here produce a unique partition of the model's explained variability. This is achieved by considering all potential model compositions given a set of explanatory variables and by accounting for model uncertainty.[1]

Third, unlike previous studies focusing on incidences, we correct the official statistical figures of the Italian Ministry of Civil Protection (MCP) in order to account for the under-reporting of cases across sample units and across time by employing the algorithms of Nishiura et al. (2009) and Russell et al. (2020). In addition, we perform a variety of sensitivity tests to verify the robustness of our findings by investigating if our results hold when we consider (i) alternative prior distributions over the parameters and the model space, (ii) a different scale for our sample units (i.e., provinces rather than regions), (iii) the role of spatial interdependence and spillovers among sample units, (iv) different time windows, and (v) unobserved regional and time heterogeneity.

The study is organized as follows. Section 2, which follows this introduction, reviews the theoretical mechanisms and the empirical evidence linking climate to COVID-19 contagions. Section 3 describes the data on regional contagion and climatic factors and provides preliminary evidence on the link between these variables. Section 4 describes the dataset used in this study and the various factors considered in the analysis. In Section 5, the BMA econometric modeling framework is presented. The empirical findings and robustness checks are presented in Section 6. Finally, Section 7 discusses the policy implications that can be derived from this research and offers the main conclusions of the study.

2 | WHY SHOULD TEMPERATURE MATTER FOR REGIONAL COVID-19 SEVERITY?

There are variety of reasons that could explain a link between temperature and regional COVID-19 severity.

First, regions with colder environments may suffer from higher COVID-19 incidence given that lower temperatures decrease metabolic functions and defense barriers in human hosts (Lowen & Steel, 2014). Second, laboratory-based evidence suggests that higher temperatures significantly reduced the effectiveness of the SARS-CoV-2 replications, whereas colder ones did not affect its infectiousness (Chan et al., 2020; World Health Organization, 2020c). A third indirect mechanism linking climate factors to contagions might involve aerosol transmission being a relevant route of COVID-19 transmission, as suggested by Morawska and Cao (2020), Morawska et al. (2020), and Zhang et al. (2020), among others. Higher temperatures can curve the efficiency of the aerosol transmission route, as they favor social interactions in outdoor spaces, where aerosol transmission of the virus is less likely to occur (Bhagat et al., 2020; Van Doremalen et al., 2020). The intuition is that in outdoor environments air circulation reduces the stagnation of dense airborne viral particle compounds and subsequent inhalation by others (Bhagat

[1]Note that, in standard statistical or econometric software packages, unless the explanatory factors are orthogonal, ANOVA decompositions of the sum of squares or the R^2 into each source of variation in the model will not be unique, and will depend on the specific ordering of variables.

et al., 2020; Miller et al., 2020). On the contrary, in colder regions a higher frequency of social interactions take place in closed spaces, where the resort to heating systems that dry out the air is more common and where ventilation is poorer. These factors increase the likelihood of evaporation of respiratory droplets and long-lasting airborne suspension of viral particles indoors, favoring the spread of the disease.

The arguments outlined above suggest a negative link between temperature and COVID-19 infections. However, the results of the strand of literature analyzing the link between temperature and COVID-19 incidence are not conclusive as they virtually fit all possibilities and reach diverging conclusions. Table 1 presents further details on the various research designs employed during 2020 and summarizes the state of the literature.

As observed, a number of studies such as Ahmadi et al. (2020), Bashir et al. (2020), Briz-Redón and Serrano-Aroca (2020), Bukhari and Jameel (2020), Pan et al. (2020), Pedrosa (2020), and Yao et al. (2020) find no evidence of any statistical relationship between temperature and infections. Other authors such as Cartení et al. (2020), Iqbal et al. (2020), Lin et al. (2020), Méndez-Arriaga (2020), Oliveiros et al. (2020), Oto-Peralías (2020), Perone (2020), Prata et al. (2020), Qi et al. (2020), Sajadi et al. (2020), Wang et al. (2020b), and Zhang et al. (2020) observe a negative effect. On the contrary, the studies of Auler et al. (2020), Kumar (2020), Ma et al. (2020), Merow and Urban (2020), and Zoran et al. (2020) suggest a positive relationship.

In summary, 15 studies find a negative and significant effect, 7 an insignificant one, and 5 a positive effect. This diversity of results is due to these contributions differing considerably in terms of the sample composition, the study period, the indicator used to measure the impact of the epidemic, and, more importantly, the statistical approach employed to perform inference. In view of this, further empirical research is required to clarify the nature of the link between climatic factors and COVID-19 incidence while tackling the problems highlighted above.

3 | DATA AND PRELIMINARY EVIDENCE

Our baseline indicator on total COVID-19 incidences was collected daily between February 24, 2020 and April 15, 2020 from the Italian Ministry of Civil Protection (MCP) at the NUTS-2 level. However, to carry out our research, we also need data on regional temperatures. Given that there is a time lag between the transmission date, the development of symptoms, the test realization, and the recording of test results later on by the authorities, we resort to a lagged value of temperatures to capture the fact that, if present, climatic effects should have taken some time to exert an impact on contagions and become visible in the data (Palialol et al., 2020; Verity et al., 2020). For this reason, we begin our analysis relating the average temperatures in February of each regional centroid to the cumulative incidences in April 15. Temperature data for each region are calculated after averaging over the time series of daily mean temperatures at 2 m above the surface of the Earth during February 2020. These meteorological data were taken from the NASA Prediction Of Worldwide Energy Resources (NASA-POWER) v8 GIS database.

Figure 1 panel (a) shows the geographical distribution of the total contagions per 100,000 inhabitants for each Italian region on April 15. Interestingly, Figure 1 shows a clear asymmetry in the geographical distribution of infections across regions. The information on temperature is shown in panel (b) of Figure 1. As observed, there is substantial variation in regional temperatures, ranging from -4° C to 10° C. As the color scale range in each panel is set to reflect a higher value of the variable being mapped, the observation of Figure 1 reveals that higher cumulative incidence levels occurred in regions with lower temperatures in February.[2]

To further investigate this link, Figure 2 provides a graphical illustration of the association between average daily temperature and COVID-19 cumulative incidence per 100,000 inhabitants by April 15. The scatter plots suggest the existence of a negative relationship between the magnitude of cumulative contagions and temperatures. This means

[2]The corresponding regional NUTS-2 codes and regional names shown in the maps are: ITC1-Piedmont, ITC2-Aosta Valley, ITC3-Liguria, ITC4-Lombardy, ITF1-Abruzzo, ITF2-Molise, ITF3-Campania, ITF4-Apulia, ITF5-Basilicata, ITF6-Calabria, ITG1-Sicily, ITG2-Sardinia, ITH1-Autonomous Province of Bolzano, ITH2-Autonomous Provincce of Trento, ITH3-Veneto, ITH4-Friuli-Venezia Giulia, ITH5-Emilia-Romagna, ITI1-Tuscany, ITI2-Umbria, ITI3-Marche, ITI4-Lazio

TABLE 1 Climatic effects and COVID-19 severity

Authors (year)	Dependent variable	Sample	Period	Methodology	Environmental controls	Other controls
Cartení et al. (2020)	New cases	20 Italian regions	February 21 to April 20	Pooled panel regression	Yes	Yes
Iqbal et al. (2020)	Total cases Death rates	210 countries	January to June 2020	Cross-section regression	No	No
Lin et al. (2020)	Doubling time cases	69 countries 11 Chinese provinces		Cross-section regression	RH	Yes
Méndez-Arriaga (2020)	Total cases LTR	31 Mexico's states and the capital	February 29 to to March 31	Correlation analysis	No	No
Oliveiros et al. (2020)	Doubling time	31 Chinese provinces	January 23 to March 11	Cross-section regression	Yes	No
Oto-Peralías (2020)	Log of total cases per capita	50 Spanish provinces	February 21 to April 1	Cross-section Step-wise	Air pollution	Yes
Paez et al. (2020)	Incidence Ratio	50 Spanish provinces	March 13 to April 11	Spatial SUR	Yes	Yes
Palialol et al. (2020)	Total cases	186 countries 416 regions	February 22 April 23	Panel fixed effects	Precipitation	No
Perone (2020)	Death rate	20 Italian regions 117 Italian provinces	February to April	Cross-section regression	RH, DTR	Yes
Prata et al. (2020)	Logarithm of new cases	27 Brazilian cities	February 27 to April 1	Panel data GAM regression	No	Yes
Qi et al. (2020)	Logarithm of new cases (MA)	31 Chinese provinces	December 2019 to February 2020	Time series GAM regression	RH	No
Sajadi et al. (2020)	Logarithm of total cases	30 × 30 km grid of cells in 50 cities of countries	January to March 10	Cross-section regression	RH	No
Wang et al. (2020b)	Reproduction number	100 Chinese cities	January 21 to January 23	Cross-section regression		
Xie and Zhu (2020)	Logarithm of new cases (MA)	122 Chinese cities	January 23 to February 29	Panel data GAM regression	RH, APR, WS	No
Zhang et al. (2020)	New cases	219 Chinese cities	January 24 to February 29	Pooled panel regression	RH, WS Air pollution	No

(Continues)

TABLE 1 (Continued)

Authors (year)	Dependent variable	Sample	Period	Methodology	Environmental controls	Other controls
Not significant						
Ahmadi et al. (2020)	Infection rate	31 Iranian regions	February 19 to March 22	Correlation analysis	No	No
Bashir et al. (2020)	New cases Total cases Mortality	New York	March 1 to April 10	Correlation analysis	No	No
Briz-Redón and Serrano-Aroca (2020)	Total cases	47 Spanish provinces	February 25 to March 25	Time series GAM regression	No	Yes
Bukhari and Jameel (2020)	Total cases	Countries	Six 10-day subperiods January 20 to March 21		No	No
Pan et al. (2020)	Reproduction number	202 locations in 8 countries	18 days after the first case	Time series	RH, WS	No
Pedrosa (2020)	Growth rate	110 countries 51 US states	10 days exp. growth after 100 cases	Cross-section	T AH	Yes
Yao et al. (2020)	Reproduction number	224 Chinese cities	January to March 9	Correlation analysis	No	No
Positive effect						
Auler et al. (2020)		5 Brazilian cities	March 13 to April 13	Principal components	RH	No
Kumar (2020)		6 India mega-cities	29 February to 30 May	Correlation Analysis	No	No
Ma et al. (2020)	Death rate	Wuhan, China	20 January to 29 February 2020	Time series GAM regression	DTR, AH, RH Air pollutants	No
Merow and Urban (2020)	Contagion growth rate	128 countries (98 states) grid of cells of 0.25 × 25 degrees	Early growth phase (prior to interventions)	Panel data		
Zoran et al. (2020)	New cases Total cases Mortality	Milan, Italy	January to April 30	Correlation analysis	No	No

Notes: RH denotes relative humidity, APR air pressure, WS wind speed, DTR day temperature range. Air pollution usually includes PM2.5, PM10, and NO2 controls. GAM refers to generalized additive models, SUR seemingly unrelated regression.

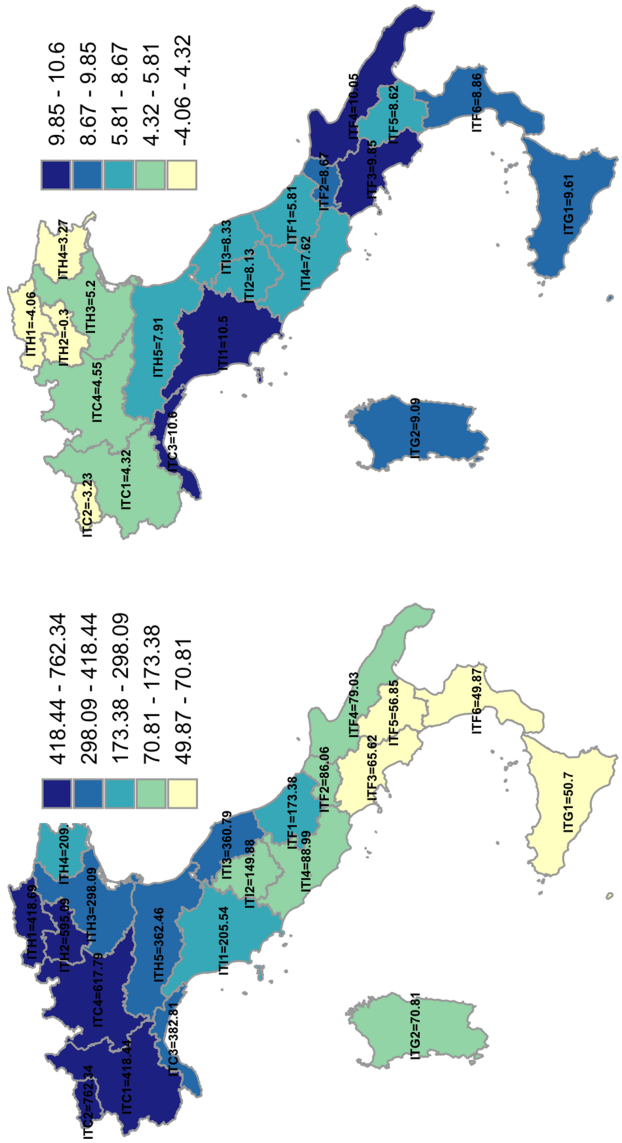

(a) Cumulative cases (b) Temperatures at February

FIGURE 1 The geographical distribution of contagions and temperatures

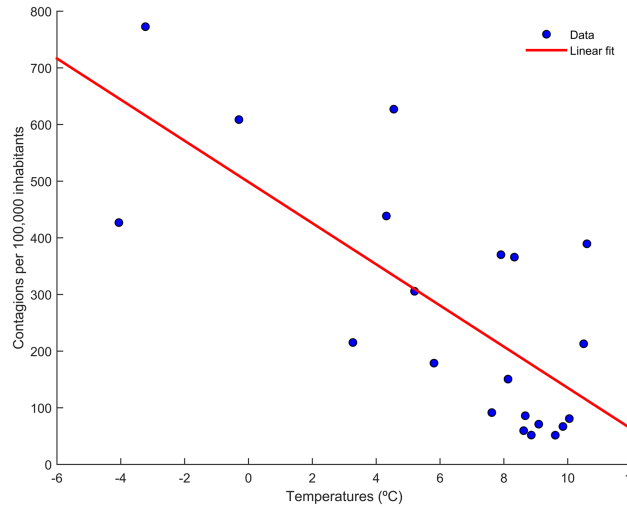

FIGURE 2 The link between temperature and COVID-19 contagions in Italian regions

that regions with higher temperatures tend to have lower levels of infection, while those regions with lower temperatures, on average, are characterized by a higher incidence. Indeed, the pairwise correlation between the two variables is statistically significant ($\rho = -0.723$ with $p = 0.00$). It is also worth mentioning that contagions and temperature both display a significant positive spatial correlation as the estimated Moran's *I* test statistic when using a 5-nearest neighbor's connectivity matrix is 0.68 ($p = 0.00$) and 0.36 ($p = 0.00$), respectively.

This evidence is in line with the arguments in Section (2). Nonetheless, the information provided by Figure 2 should be treated with caution, as the observed connection between temperature and regional epidemic size may simply be a spurious correlation resulting from an ecological fallacy (Ghosh & Cartone, 2020) or the omission of other variables affecting both climate and infections. In view of this potential problem, in Section (5), we develop a more appropriate statistical analysis on the link between temperatures and regional COVID-19 cases.

4 | THE POTENTIAL DRIVERS OF COVID-19 CONTAGIONS

With the aim of (i) analyzing the robustness of the relationship between temperature and COVID-19 incidence, (ii) producing a comprehensive ranking on the importance of the determinants of contagions, and (iii) minimizing the risk of biased estimates due to omitted variables in the specification of the model, we consider a variety of candidate factors that could explain regional disparities in the severity of incidence and that may be correlated with temperatures.

We now describe these controls, which are also collected at the NUTS-2 level and provide a brief conceptual justification for their inclusion in the analysis. Table 2 presents the detailed definition and the sources of all the control variables used in the paper.

4.1 | Climate and environmental factors

The first group of factors that are likely to explain regional disparities refers to the climate and the environmental conditions of the region. Besides the potential role of (i) *temperature*, which is the key variable of interest

TABLE 2 Data, variable definitions, and sources

Variable	Variable definition	Source	Date
Contagions	Total COVID-19 contagions per 100,000 inhabitants on April 15	MCP	2020
Contagions (corrected)	Total COVID-19 contagions per 100,000 inhabitants on April 15	Own elaboration	2020
	corrected for under-reporting as in Russell *et al*. (2020)		
A. Climate, environment and geography			
Mean temperatures	Average mean daily temperature at 2 meters above the surface during February 2020	NASA-POWER v8	2020
Relative humidity	Average of the mean daily relative humidity at 2 meters above the surface during February 2020	NASA-POWER v8	2020
Solar radiation(a)	Average of the mean daily solar radiation incident on a horizontal surface for all sky conditions	NASA-POWER v8	2020
Air pollution	Percentage of population exposed to more than 15 $\mu g/m^3$ of PM.2.5 particles	OECD	2020
Distance to the epicenter	Distance in kilometers from Lombardy (regional centroid distances)		
B. Economic and political factors			
Policy lags	Number of days elapsed between 1 infection per 100,000 inhabitants and the lockdown	Own elaboration	2020
Health spending	Health spending (in % of GDP)	Statista, Eurostat	2019
Quality of government	Regional quality of government index based on the indicators of corruption,	Charron *et al*. (2014)	2017
	regulatory quality, and impartiality		
Tests	Number of COVID-19 tests performed per 100,000 inhabitants from February 24 to March 1	MCP	2020
C. Demographic factors			
Share of young	Share of population aged between 0 and 35 years old	Eurostat	2019
Share of elderly	Share of population aged above 75 years old	Eurostat	2019
	(iii) Diseases of the circulatory system (per 100,000 inhabitants)		
D. Social connectedness			
Infrastructure density	Number of kilometers of motorways and railways network per squared kilometer	Eurostat	2018
Population density	Population per squared kilometer	Eurostat	2018
Social mobility	Average municipal commuting flows (incoming and outgoing) relative to the population employed	Pluchino *et al*. (2020)	2020

Notes: MCP Ministry of Civil Protection, NASA-Prediction Of Worldwide Energy Resources (NASA-POWER) v8 GIS database. The variables and data sample employed in the baseline analysis are taken at the NUTS-2 level.

and whose potential effects have already been discussed in Section (2), another climatic factor that has received considerable attention in the literature is that of (ii) *relative humidity* (Bashir et al., 2020; Lin et al., 2020; Pan et al., 2020; Qi et al., 2020). Although the existing evidence is mixed, we expect regions with lower relative

humidity to have a lower incidence, as humidity decreases the stability of airborne viral particles (Lowen & Steel, 2014).[3]

A third factor is (iii) *air pollution*, as it may exacerbate the vulnerability of populations by worsening chronic lung infections (Cui et al., 2003). Another potential channel for a positive link is that airborne particles may have been able to serve as carrier for the pathogen (Yongjian et al., 2020; Zoran et al., 2020). In the context of the COVID-19 analysis, some studies suggest that particulate matter pollution tends to increase contagions and subsequent health damages (Bashir et al., 2020; Cartení et al., 2020; Perone, 2020; Wu et al., Yongjian et al., 2020). In our empirical analysis, we control for the impact of air pollution by means of the share of population that is exposed to more than 15 μg/m^3 of particulate matter (PM2.5) using data from the OECD regional database.

We also consider the role played by (iv) the *distance to the epicenter* of the epidemic, which in Italy occurred in Lombardy. In an analogy with the diffusion of the impacts of an earthquake, we expect that a higher distance to the epicenter of the pandemic may have reduced the share of imported contagions and the final epidemic size in other regions. This intuition is supported by the works of Fang and Wahba (2020) or Oto-Peralías (2020), where distance to Wuhan (China) and Madrid (Spain) is observed to be an important predictor of contagion differentials. Furthermore, controlling for distances to Lombardy is relevant in the Italian context, given that regions in the south of the country or in the Mediterranean islands, located far away from Lombardy, tend to have better climatic conditions.

In addition, we examine the possible effects of (v) *solar radiation*. Solar radiation contains ultraviolet (UV) radiation (Merow & Urban, 2020), which is deemed to degrade viral genetic material. An additional reason to believe that solar radiation could decrease infections is that it travels together with sunlight, which has been shown to increase human host defenses through enhanced production of vitamins (Cannell et al., 2006; Martineau et al., 2017). Controlling for these factors is relevant in this context as they are highly correlated with temperature.

4.2 | Health policy factors

Regional differences in health policy might also be responsible for the differences in the severity of the epidemic. The first variable considered in this regard is (vi) the number of *tests*, given that a higher ability of regional authorities to detect infections in an early stage may have helped to decrease contagions. The reason is that an early and correct diagnosis of the infection may have helped to identify potential carriers, isolate them properly, and reduce higher-order transmission chains (Cartení et al., 2020; Romer, 2020; Wang et al., 2020a). To operationalize this variable, we calculate the number of tests performed by 100,000 inhabitants during the first week of the epidemic outbreak. The second health policy factor considered is (vii) the *'policy lag'*, or the delay in the application of regional lockdowns to limit viral transmission. Because the number of new cases was growing at an exponential rate in the early stages of the outbreak, time lags in the adoption of the regional lockdown of regions relative to the stage of the epidemic outbreak may have helped to increase diffusion and the epidemic size (Alvarez et al., 2020; Orea and Alvarez, 2020). We define the policy lag as the number of days elapsed between one infection per 100,000 inhabitants and the day of the lockdown. We also control for the regional variability in (viii) *health spending*, measured in percentage of the gross domestic product (GDP), because regions with a higher expenditure should have experienced fewer shortages of equipment and educated manpower for testing, implementing contact tracing and locating cases, carrying out treatments, and minimizing within-hospital contagion amplification (Kapitsinis, 2020; Lin et al., 2020; Perone, 2020).

Finally, we account for differences in (ix) the regional *quality of government* using the European Quality of Government Index (EQI), developed by (Charron et al., 2014). In the context of a health crisis, a higher quality of government is expected to influence the quality of health care services but also the adaptability of institutions to

[3]Relative humidity (RH) indicates the state of absolute humidity relative to a maximum humidity given the same temperature. We use data from the (NASA-POWER) v8 GIS database.

a changing and turbulent environment (Ezcurra & Rios, 2019; Rios & Gianmoena, 2020), helping to buffer the epidemic shock.

4.3 | Demographic factors

Sociodemographic factors may also play a relevant role determining reported infections (Andersen et al., 2020; Cartení et al., 2020; Prata et al., 2020). To control for differences in the demographic structure, we consider (x) the *share of young* population, measured as share of population under 35 years old, and (xi) the *share of elderly* population, measured as the share of population above 75 years old. Given that there is evidence that effects of COVID-19 are much more severe in older populations (Verity et al., 2020) and because of the limited ability to perform tests on the population, regional authorities may have prioritized detection among the elderly over the the younger groups (who in many cases could have been asymptomatic carriers). For this reason, we expect regions with a higher share of elderly population to have reported more cases per capita than regions with a younger population.

4.4 | Social connectivity factors

Finally, we control for the fact that different degrees of social connectivity could also have an impact in the spread of the disease and the probability of importing infections from abroad (Charaudeau et al., 2014). To that end, we include a proxy of (xii) the *social mobility* of the population, which takes into account the average inflows and outflows relative to the population employed. Higher levels of social mobility are expected to increase contagions (Arenas et al., 2020; Pluchino et al., 2021).

A second candidate factor in this group is the (xiii) *population density*. Because of the transmission of SARS-CoV-2 through the population operates through close person-to-person contact, compared with low-density areas, a higher population density could favor interaction and personal contacts, reinforcing the transmission of the virus (Andersen et al., 2020; Cartení et al., 2020; Oto-Peralías, 2020). Nevertheless, this argument should be taken with caution, as some extremely dense cities, such as Singapore, Seoul, and Shanghai, have outperformed many other less-populated places in combating the coronavirus. As a point of fact, Fang and Wahba (2020) or Perone (2020) find no statistical relation between density and contagions.

Finally, we consider the potential effect of (xiv) *infrastructure density*, measured as the number of road and railway kilometers per squared kilometer. This variable is expected to capture differences in the degree of connectedness of the region. Regions with large cities and large transport nodes with a massive influx of tourism and travelers should have a bias to attract epidemic outbreaks. Likewise, the use of public transport without protective equipment may have been a key factor in the rapid spread of COVID-19 (Kapitsinis, 2020; Morawska et al., 2020; Morawska & Cao, 2020).

5 | ECONOMETRIC STRATEGY

In empirical COVID-19 research, cross-sectional, time-series and generalized additive regression models approaches have been frequently employed. Nevertheless, most studies use a minimal fraction of the information in the dataset and understate real uncertainty associated with the specification of the empirical model (see Moral-Benito, 2015; Steel, 2020). To address this concern, in our analysis of the drivers of COVID-19 regional differentials, we employ a Bayesian model averaging (BMA) approach and relative importance metrics (RIM) within the context of multiple linear regression models:

$$y = \alpha\iota_n + X\beta + \epsilon \tag{1}$$

where y denotes a $N \times 1$ dimensional vector consisting of observations for the cumulative total infections per capita during February 24 to April 15, for each region $i = 1,...,N$. α reflects the constant term, ι_n is a $N \times 1$ vector of ones, X is an $N \times K$ matrix of regional explanatory variables with associated response parameters β contained in a $K \times 1$ vector. Finally, $\epsilon = (\epsilon_1,...,\epsilon_N)'$ is a vector of i.i.d disturbances whose elements have zero mean and finite variance σ^2.

5.1 | Bayesian model averaging

BMA techniques haven been previously analyzed to investigate the determinants of complex processes, and a large literature on BMA in regression models already exists (see Moral-Benito, 2015 and Steel, 2020 for detailed reviews on the literature).

However, to get an intuition behind the BMA approach employed here to understand the nature of COVID-19 regional disparities, notice that, for any set of possible explanatory variables of size K, the total number of possible models M_k is 2^K and $k \in \left[0, 2^K\right]$. This implies there are 2^K substructures of the model in Equation 1 given by subsets of coefficients $\eta^k = (\alpha, \beta^k)$ and combinations of regressors X_k, which in our context implies the model space has 16,384 candidate models.

Model averaging techniques solves the question of estimating variable importance and the effects of each regressor h by considering all the candidate models implied by the combinations of regressors in X and computing a weighted average of all the estimates of the corresponding parameter of X_h (where the subindex h here denotes a single regressor and not a model or a combination of regressors k). By proceeding in this way, model-averaged estimates consider both the uncertainty associated with the parameter estimate conditional on a given model, but also the uncertainty of the parameter estimate across different models.

By following the Bayesian logic, the posterior for the parameters η_k calculated using model M_k is written as:

$$g(\eta_k|y,X,M_k) = \frac{f(y,X|\eta_k,M_k)g(\eta_k|M_k)}{f(y,X|M_k)} \tag{2}$$

where $g(\eta_k|y,X,M_k)$ is the posterior, $f(y,X|\eta_k,M_k)$ is the likelihood and $g(\eta_k|M_k)$ is the prior. The key metrics in BMA analysis are the posterior mean (PM) of the distribution of η:

$$E(\eta|y,X) = \sum_{k=1}^{2^K} E(\eta_k|M_k,y,X)p(M_k|y,X) \tag{3}$$

and the posterior standard deviation (PSD):

$$PSD = \sqrt{Var(\eta|y,X)} \tag{4}$$

where the $Var(\eta|y,X)$ is given by:

$$\begin{aligned} Var(\eta|y,X) = \ & \textstyle\sum_{k=1}^{2^K} Var(\eta_k|M_k,y,X)p(M_k|y,X) + \\ & \textstyle\sum_{k=1}^{2^K} (E(\eta_k|M_k,y,X) - E(\eta|y,X))^2 p(M_k|y,X) \end{aligned} \tag{5}$$

To derive these metrics, it is necessary to calculate the posterior model probability $p(M_k|y,X)$ of each of the submodels M_k. These can be obtained as:

$$p(M_k|y,X) = \frac{p(y,X|M_k)p(M_k)}{\sum_{k=1}^{2^K} p(y,X|M_k)p(M_k)} \tag{6}$$

where $p(y,X|M_k)$ is the marginal likelihood and $p(M_k)$ is the prior model probability. The marginal likelihood of a model k is calculated as:

$$p(y,X|M_k) = \int_0^{\infty}\int_{-\infty}^{\infty} p\left(y,X|\eta_k,\sigma^2,M_k\right)p\left(\eta_k,\sigma^2|g\right)d\eta d\sigma \tag{7}$$

where $p\left(y,X|\eta_k,\sigma^2,M_k\right)$ is the likelihood of model k and $p\left(\eta_k,\sigma^2|g\right)$ is the prior distribution of the parameters in model M_k conditional to g, the Zellner's g-prior.

In addition, the BMA framework can be extended to generate probabilistic on the relevance of the various regressors, using the posterior inclusion probability (PIP) for a variable h:

$$p(\eta_h \neq 0|y,X) = \sum_{k=1}^{2^K} p(M_k|\eta_h \neq 0,y,X) \tag{8}$$

and the conditional posterior positivity of h:

$$p(\eta_h \geq 0|y,X) = \sum_{k=1}^{2^K} p\left(\eta_{k,h}|M_k,y,X\right)p(M_k|y,X) \tag{9}$$

where values of conditional positivity close to 1 indicate that the parameter is positive in the vast majority of considered models and values close to 0 indicate the effect on the dependent variable is negative. The calculation of previous metrics in the BMA approach requires priors on the model space and priors on the parameter space to be defined. To that end, we use a model specific Zellner g-prior based on the Bayesian risk inflation criterion (BRIC), whereas we use a calibrated binomial prior on the model space to give the same a priori probability to each model and variable. In particular, the g-prior hyper-parameter takes the value of $g_k = max\left\{N,K^2\right\}$ such that $g(\eta_k) \sim N\left[0,\sigma^2 g\left(X_k' X_k\right)^{-1}\right]$. The binomial prior on the model space regulates prior model probabilities according to $p(M_k) = \phi^k(1-\phi)^{K-k}$, where each covariate k is included in the model with a probability of success ϕ. We set $\phi = 0.5$, which implies a prior model size of 7 regressors. To draw models from the model space, we use a Markov Chain Monte Carlo Model Composition (MC^3) sampler with reversible jump (see Zeugner & Feldkircher, 2015).

5.2 | Relative importance metrics

Given that the reliability of the PIPs obtained from small samples sizes can be adversely affected by collinearity and by model sampling variability (Ghosh & Ghattas, 2015), we complement the probabilistic importance ranking provided by the PIPS within the BMA framework by computing relative importance metrics. The term relative importance here refers to the contribution that a variable makes to the prediction of contagions by itself and in combination with other predictor variables, which differs from classical statistical inference where a variable may explain only a small proportion of predictable variance and yet be considered very meaningful (Johnson & LeBreton, 2004). It also differs from the Bayesian notion of variable importance where a variable increases its importance if it usually enters into high-probability models.

To understand the intuition behind this approach, recall that, in the context of a cross-sectional regression, with $n = 1,\ldots,N$ sample units, the R^2 informs on the model's explained variability across spatial units (regions). Thus, decompositions on the relative importance of a factor X_h tell us the percentage of explained disparities across spatial

units due to factor h. In a linear regression framework with K explanatory factors, the variance of the model is given by:

$$var(y) = \sum_{h=1}^{K} \beta_h^2 v_h + 2\sum_{h=1}^{K-1}\sum_{j=h+1}^{K} \beta_h \beta_j \sqrt{v_h v_j}\rho_{j,h} + \sigma^2 \tag{10}$$

where β_h stands for the parameter of variable h, v_h for the regressor variance, $\rho_{j,h}$ is the inter-regressor correlations, and σ^2 denotes the unexplained variance. As explained by Gromping (2007), variable importance methods that decompose R^2, have to decompose the explained variance of the model (i.e, the first two summands above). However, these variances can only be uniquely partitioned in the case of uncorrelated regressors. Whenever $\rho_{j,h} \neq 0$, different methods lead to different results.

Given that the increase in the R^2 allocated to a certain factor X_h depends on which other variables are already in the model when X_h is added to be part of the explanation, Gromping (2007) propose to use the Lindeman–Merenda–Gold method, which consists of averaging such order-dependent R^2 allocations over all $p!$ orderings to produce a fair unique assessment of importance. The proportional marginal variance decomposition (PMVD) approach proposed by Feldman (2005) is a modified version with data-dependent weights penalizing variables that are not statistically significant. Others, like Zuber and Strimmer (2010, 2011), have proposed to bypass the need of estimating all possible models by decorrelating the variables with a Mahalanobis transformation and suggest to look directly at Correlation-Adjusted (marginal) coRelation (CAR) scores, whereas Genizi (1993) proposed a similar metric that can be viewed as the weighted average of squared CAR scores.

To study the relative contribution of the various factors affecting contagion, we employ the average R^2 decomposition of the various metrics discussed above. The specific formulas employed to obtain the decompositions implied by these metrics are provided in the Appendix.

6 | RESULTS

6.1 | Main results

Table 3 reports the results obtained from the BMA analysis. We use the PIPs of the different variables to classify evidence of robustness of the different contagions drivers, such that predictors with PIPs above the a priori inclusion probability (APIP = 0.5) are considered as relevant determinants and variables with PIP < 0.5 as irrelevant ones. From a Bayesian perspective, variables with PIPs higher than others reflect a higher importance as they are more likely to be part of the DGP, and as such, they can be considered as a relevant piece in explaining contagion differentials across Italian regions.

As observed in column (1) of Table 3, there is a small group of variables forming the group of important determinants. These are the mean temperatures (92%) and the policy lags (53%), which are both statistically significant at the 1% level. We also find a statistically significant effect of the distance to the epicenter of the epidemic and the relative humidity controls, although their PIPS are below the 0.5 threshold.[4] Importantly, none of the other remaining

[4]As an alternative candidate to the geographical distance with respect to Lombardy, we have experimented with a metric of economic distance based on the inverse of the GDP cross-products between Lombardy and other regions. The reason for this check is that one could expect the regions of Lombardy, Emilia-Romagna, and Lazio to be more intensely connected among themselves than Lombardy to other smaller but closer regions, making the economic distance more relevant in this context than the geographic one. However, after some experimentation, we did not find this metric to outperform the geographical distance in terms of PIPs, and its inclusion within the set of candidate explanatory factors did not alter the findings regarding the role of temperature. The results of this check can be provided upon request.

TABLE 3 Main results: Bayesian model averaged estimates

	PIPs (1)	Cond. post. Effects (2)	Cond. post. Standardized (3)	Pos. sign Positivity (4)	Expected Effect (5)	R^2 (%) (6)
Temperature	0.92	-29.423***	-0.59***	0.00	-	30
		(9.138)	(0.18)			
Policy lag	0.53	26.040***	0.47***	0.99	+	12.4
		(10.335)	(0.18)			
Distance to epicenter	0.47	-0.395**	-0.55**	0.00	-	16.3
		(0.164)	(0.23)			
Relative humidity	0.29	-11.990**	-0.21**	0.00	-	3.9
		(6.571)	(0.11)			
Tests	0.17	-1.474	-0.19	0.01	-	2.3
		(1.159)	(0.14)			
Health spending	0.12	-28.537	-0.25	0.24	-	8.9
		(39.38)	(0.34)			
Share of elderly	0.09	-4.917	-0.03	0.40	+	1.9
		(31.80)	(0.23)			
Social mobility	0.09	7.788	0.11	0.75	+	6.7
		(16.919)	(0.24)			
Population density	0.08	0.172	0.05	0.88	+	1.4
		(1.844)	(0.18)			
Share of young	0.08	-4.658	-0.04	0.32	-	1.5
		(23.220)	(0.22)			
Air pollution	0.08	0.104	0.01	0.56	+	1.8
		(0.332)	(0.16)			
Quality of government	0.08	0.357	0.02	0.38	-	6.3
		(4.321)	(0.25)			
Infrastructure density	0.07	-30.156	0.02	0.59	+	1
		(155.776)	(0.16)			
Solar radiation	0.07	0.131	-0.05	0.43	-	5.6
		(1.127)	(0.23)			

Notes: The dependent variable in all regressions is the total number of contagions per 100,000 inhabitants from the Italian CPM. The results reported correspond to the estimation of all the models in the model space including any combination of the 14 variables. We use a fixed BRIC *g*-prior on the parameters and a binomial model prior with prior mean model size equal to 7 in all cases. Variables are ranked by column (1), the posterior inclusion probability. Columns (2) and (3) reflect the conditional posterior mean and the standardized conditional posterior mean for the linear marginal effects of each variable, respectively. Column (4) is the sign certainty probability, a measure of our posterior confidence in the sign of the coefficient. Column (5) shows the expected effect in line with the analysis of the potential determinants in Section (4). Column (6) reports the averaged share of the model's R^2 attributed to each variable when calculating the LMG, CAR, GEN, and PMVD relative importance metrics decompositions. Standard deviations in parentheses. * Significant at 10% level, ** significant at 5% level, *** significant at 1% level.

factors considered appears to be relevant in explaining regional differentials across Italian regions from either a Bayesian/frequentist perspective, even if they mostly display the expected signs and, in general, appear to be mostly consistent with those obtained in the literature.

Therefore, we do not find evidence supporting many of the often-hypothesized environmental, health, or demographic drivers of COVID-19 severity to be of first-order importance in the Italian context.[5]

The robustness of the link between temperature and COVID-19 incidence is confirmed when looking at the decomposition of the R^2 of the model in column (6). The R^2 of the model when including all factors is 89%. Therefore, with the set of factors considered, we are able to account for most of the variability observed in the data. As shown, temperature is a relevant factor explaining 30% of NUTS-2 level regional contagion differentials followed by the policy lags variable and distance to Lombardy, which explain 12.4% and 16.3% of the regional variability, respectively. In sum, our findings suggest that, by focusing on the role played by climate conditions, policy lags, and the distance to Lombardy, we have most of the information needed to explain why some regions may have been more severely affected than others.

We now turn our attention to the model-averaged estimates of the effects of our regional-level determinants as they provide the basis for posterior inference. Model-averaged estimates of the effect of each variable conditional to inclusion are reported in columns (2) and (3) constructed using a sampler over the 16,384 possible model combinations implied by our set of variables and by computing a probabilistic weighted average of all the estimates of the corresponding parameter. As regards our variable of interest, we find that temperature exerts a negative impact on regional contagion outcomes with a posterior mean of -29.423 and a standardized effect of -0.59 standard deviations. This means that an increase in 1 degree Celsius in the mean regional temperature during February decreased the number of total contagions per 100,000 inhabitants on April 15 by 29,423. Alternatively, the estimated standardized posterior mean coefficient in column (3) reveals that, on average, a 1 standard deviation shock to the temperatures (i.e., a change of about 4.3 degrees Celsius, which is the difference in the temperatures between the average temperatures of Lombardy [ITC4] and Calabria [ITF6]) may have had the effect of decreasing the total number of contagions per 100,000 inhabitants by 126.5, which is the difference between the highly affected region of Piedmont (ITC1) and that of Veneto (ITH3). Moreover, as shown in column (4), the posterior sign positivity of the temperatures is 0.00%, which implies the parameter estimate is always negative irrespective of the model in which the variable appears.

It is also worth mentioning that the finding of a positive and statistically significant impact on the number of infections due to a late political response is in line with the results obtained in other studies (Alvarez et al., 2020; Orea & Alvarez, 2020). Specifically, we find that each additional day in which the lockdown was not implemented, with respect to the detection date of one case per 100,000 inhabitants, meant an increase of 26.040 cases per 100,000 inhabitants by April 15. To put this figure in context, this estimates imply that, in Lombardy (ITC4), implementing the full lockdown on March 1 instead of March 8 would have decreased the total amount of cases by 33%, decreasing the incidence toll from 62,153 cases to 41,435 cases.

6.2 | Sensitivity analysis

We now investigate if the finding of temperature being a key determinant of contagion differentials across Italian regions is robust to changes in the setup of the analysis.

[5]Among the group of regressors with low PIPS, it is worth mentioning the estimated posterior mean of solar radiation is not statistically different from zero and the posterior sign seems to change considerably among the set of models drawn by the MC^3 sampler. This finding may seem at odds with the negative link for temperature, since temperature and solar radiation are clearly interlinked. However, note that after controlling for cross-sectional temperature variation our solar radiation indicator should not capture infrared radiation variation anymore but mostly UV radiation differentials, which are not related to temperature. Therefore, the theoretical mechanism of solar UV radiation degrading viral material does not seem to be relevant to explain regional incidence disparities in Italy.

6.2.1 | Alternative coordinates

We first explore the sensitivity of our results with respect to the set of coordinates in which we measure our climatic variables. In our baseline analysis, we have used the latitude and longitude of the centroids of each region. However, it could be argued that the relevant temperatures are not those of the regional centroid but those in which there is a greater population and economic activity. Therefore, we now analyze whether the results change when using the geographical coordinates of the most populated city within the region to compute our climate factors. The results from this robustness check are presented in Table 4. As can be seen, the findings are similar to our benchmark given that temperature appears as the factor with higher PIPs (96%) and a negative and statistically significant effect.

6.2.2 | Alternative prior distributions

An implication of the Bayesian model averaging approach is that inferences drawn on the effects of the various factors and their importance depend on prior distributions assigned to the model parameters and on the model space. Thus, we analyze if the results regarding the probabilistic importance of the variables are driven by the prior distributions employed so far. Table 5 serves that purpose.

We check the sensitivity of our results to the definition of the baseline binomial prior on the model space, with $\phi = 0.5$. Hence, we depart from the baseline specification, and we set the prior model size to 7, 8, 9, and 10 regressors respectively, by adjusting ϕ in each case. Secondly, we consider a variety of different g-priors specifications on the parameters while holding fixed $\phi = 0.5$, which are implemented following Zeugner and Feldkircher (2015). As shown in Table 5, the effect of increasing the prior model size has a stronger effect on the PIPs than changing the g-prior, since the employment of priors favoring large model sizes increases slightly the PIPs of most of the potential determinants. Nevertheless, the results obtained confirm the results are not driven by priors, as it is clear that temperature and policy lags are always the top drivers.

6.2.3 | Alternative scale of analysis

A third concern with the validity of previous results is that they may suffer from so-called modifiable areal unit problem (MAUP). The MAUP is a form of ecological fallacy associated with the aggregation of data into areal units for geographical analysis such that the original underlying spatial patterns between variables may be distorted when measured at other levels (Openshaw, 1984), and there is evidence that it can occur in COVID-19 analysis in Italy (Ghosh & Cartone, 2020). [6]

Thus, to verify that our results on the link between temperature and COVID-19 severity are robust to a potential data aggregation bias, we now check if the previously observed negative effect holds at a higher level of geographical resolution. In Table 6, we report the BMA results obtained when using a more disaggregated dataset consisting of 107 Italian provinces and when using provincial level regressors whenever possible.

We begin by discussing the main points of this check regarding the role of temperature. First, the core set of regressors conforming the group of 'top drivers' of provincial COVID-19 severity is similar to that of our benchmark regional level. This group consists of the degree of social mobility (99%), followed by the distance to the epicenter (96.8%) (i.e., the province of Lodi), the provincial relative humidity (93.6%), the provincial temperatures

[6]As shown in Figures A2 and A3 in the Appendix, (i) the negative correlation at the provincial level is lower $\rho = -0.51$ and (ii) there is a significant degree of variation in temperature within regions. In fact, the provincial coefficients of variation for temperature and cumulative incidence within regions are 0.209 and the 0.443, respectively, which suggests that both temperature and COVID-19 incidence experience a significant degree of variation at lower levels of disaggregation.

TABLE 4 Alternative set of coordinates for climatic factors

	PIPs (1)	Cond. post. Effects (2)	Cond. post. Standardized (3)	Pos. sign Positivity (4)	Expected Effect (5)	R^2 (%) (6)
Temperature	0.96	-30.222***	-0.664***	0.000	-	30.4
		(8.22)	(0.18)			
Relative humidity	0.80	-17.486***	-0.314***	0.000	-	6.5
		(6.45)	(0.12)			
Policy lag	0.66	25.836***	0.466***	0.997	+	11.1
		(10.31)	(0.19)			
Social mobility	0.33	23.762	0.335	0.988	+	9.8
		(14.55)	(0.21)			
Distance to epicenter	0.29	-0.315	-0.438	0.001	-	10.1
		(0.20)	(0.28)			
Share of elderly	0.17	-15.067	-0.110	0.222	+	1.2
		(31.16)	(0.23)			
Population density	0.16	0.280	0.151	0.956	+	1.5
		(0.33)	(0.18)			
Health expenditure	0.13	-20.430	-0.175	0.108	-	9.6
		(32.67)	(0.28)			
Solar radiation	0.12	18.952	0.109	0.806	-	6.2
		(42.02)	(0.24)			
Air pollution	0.12	0.677	0.058	0.770	+	2.4
		(1.74)	(0.15)			
Quality of government	0.12	2.072	0.120	0.815	-	7.5
		(4.46)	(0.26)			
Share of young	0.11	-3.025	-0.029	0.569	-	1.6
		(22.10)	(0.21)			
Tests	0.10	-0.485	-0.061	0.140	-	1.0
		(1.13)	(0.14)			
Infrastructure density	0.10	-0.120	-0.017	0.402	+	0.9
		(1.14)	(0.16)			

Notes: The dependent variable in all regressions is the total number of contagions per 100,000 inhabitants from the Italian MCP measured at the regional NUTS-2 level. Climatic factors such as temperature, relative humidity, and solar radiation are measured at the coordinates of the most populated city within the region rather than in the regional centroid. The results reported correspond to the estimation of all the models in the model space including any combination of the 14 variables. We use a fixed BRIC *g*-prior on the parameters and a binomial model prior with prior mean model size equal to 7 in all cases. Variables are ranked by column (1), the posterior inclusion probability. Columns (2) and (3) reflect the conditional posterior mean and the standardized conditional posterior mean for the linear marginal effects of each variable, respectively. Column (4) is the sign certainty probability, a measure of our posterior confidence in the sign of the coefficient. Column (5) reports the averaged share of the model's R^2 attributed to each variable when calculating the LMG, CAR, GEN, and PMVD relative importance metrics decompositions. Standard deviations in parentheses. * Significant at 10% level, ** significant at 5% level, *** significant at 1% level.

(75%), and the policy lags in the adoption of the lockdown (57.6%). Second, when looking at the the decomposition of the R^2 of the model, we find that temperature appears in the third place of importance, explaining 13.5% of the provincial variability in COVID-19 severity, just below the distance to the epicenter (22.3%) and mobility

TABLE 5 Alternative prior distributions

	Model size = 7		Model size = 8		Model size = 9		Model size = 10	
	Prior	Posterior	Prior	Posterior	Prior	Posterior	Prior	Posterior
Temperature	0.50	0.92	0.57	0.95	0.64	0.96	0.71	0.97
Policy lag	0.50	0.53	0.57	0.58	0.64	0.63	0.71	0.70
Distance to epicenter	0.50	0.48	0.57	0.46	0.64	0.46	0.71	0.45
Relative humidity	0.50	0.29	0.57	0.37	0.64	0.47	0.71	0.58
Tests	0.50	0.17	0.57	0.23	0.64	0.31	0.71	0.43
Health spending	0.50	0.12	0.57	0.13	0.64	0.16	0.71	0.19
Share of elderly	0.50	0.09	0.57	0.12	0.64	0.17	0.71	0.24
Social mobility	0.50	0.09	0.57	0.12	0.64	0.15	0.71	0.21
Air pollution	0.50	0.09	0.57	0.11	0.64	0.14	0.71	0.18
Share of young	0.50	0.08	0.57	0.11	0.64	0.14	0.71	0.18
Population density	0.50	0.08	0.57	0.11	0.64	0.14	0.71	0.18
Quality of government	0.50	0.08	0.57	0.10	0.64	0.13	0.71	0.17
Solar radiation	0.50	0.08	0.57	0.09	0.64	0.13	0.71	0.16
Infrastructure density	0.50	0.07	0.57	0.09	0.64	0.12	0.71	0.17
	EBL		Hyper-g		EBL		RIC	
	Prior	Posterior	Prior	Posterior	Prior	Posterior	Prior	Posterior
Temperature	0.50	0.91	0.50	0.87	0.50	0.95	0.50	0.93
Policy lags	0.50	0.66	0.50	0.62	0.50	0.67	0.50	0.55
Relative humidity	0.50	0.57	0.50	0.56	0.50	0.56	0.50	0.33
Distance to epicenter	0.50	0.49	0.50	0.51	0.50	0.47	0.50	0.47
Tests	0.50	0.47	0.50	0.47	0.50	0.43	0.50	0.20
Share of elderly	0.50	0.34	0.50	0.37	0.50	0.27	0.50	0.10
Social mobility	0.50	0.32	0.50	0.35	0.50	0.25	0.50	0.10
Health spending	0.50	0.31	0.50	0.35	0.50	0.24	0.50	0.12
Population density	0.50	0.31	0.50	0.35	0.50	0.23	0.50	0.10
Share of young	0.50	0.30	0.50	0.34	0.50	0.23	0.50	0.10
Air pollution	0.50	0.30	0.50	0.33	0.50	0.23	0.50	0.10
Quality of government	0.50	0.29	0.50	0.33	0.50	0.22	0.50	0.09
Infrastructure density	0.50	0.29	0.50	0.33	0.50	0.22	0.50	0.08
Solar radiation	0.50	0.28	0.50	0.33	0.50	0.21	0.50	0.09

Notes: The dependent variable in all regressions is the total number of contagions per 100,000 inhabitants from the Italian MCP. The results reported correspond to the estimation of all the models in the model space including any combination of the 14 variables. Model specific g-prior distributions differ from our baseline g-prior, the BRIC, which sets $g = max\left(N; K^2\right)$. In this group of g-prior distributions, we consider the (i) empirical Bayes prior (EBL) which is a model k specific g-prior estimated via maximum likelihood. In this case $g = max(0, F_k)$ where $F_k = \frac{R_k^2(N-1-k)}{\left(1-R_k^2\right)}$. (ii) We consider also the hyper-g prior, which relies on a beta prior on the shrinkage factor of the form $\frac{g}{1+g} \sim Beta\left(1, \frac{a}{2} - 1\right)$ where, in this specific case, $a = 3.5$. In addition, we consider the (iii) unit information prior (UIP), which sets $g = N$, and the (iv) risk information criteria prior (RIC) where $g = K^2$.

TABLE 6 Provincial-level results: Bayesian model averaged estimates

	PIPs (1)	Cond. post. Effects (2)	Cond. post. Standardized (3)	Pos. sign Positivity (4)	Expected Effect (5)	R^2 (%) (6)
Social mobility	0.99	1.802***	0.36***	1.00	+	18.5
		(0.430)	(0.08)			
Distance to epicenter	0.96	-0.36***	-0.43***	0.00	-	22.3
		(0.12)	(0.14)			
Relative humidity	0.95	-14.677***	-0.20***	0.00	-	4.8
		(4.60)	(0.06)			
Temperature	0.75	-16.839***	-0.22**	0.00	-	13.5
		(7.18)	(0.08)			
Policy lag	0.54	13.119**	0.17**	1.00	+	10.27
		(5.70)	(0.08)			
Reg. tests	0.51	-1.391**	-0.16**	0.00	-	2
		(0.65)	(0.07)			
Population density	0.44	-0.100**	-0.13**	0.00	+	1.3
		(0.05)	(0.07)			
Share of young	0.31	27.259	0.14	0.99	-	0.9
		(16.34)	(0.09)			
Share of elderly	0.16	-8.772	-0.05	0.21	+	0.8
		(14.82)	(0.13)			
Reg. quality of government	0.13	2.580	0.010	0.94	-	7.4
		(2.79)	(0.11)			
Reg. health spending	0.13	12.871	0.10	0.91	-	7.2
		(23.19)	(0.16)			
Reg. infrastructure density	0.12	0.467	0.06	0.99	+	3.5
		(0.80)	(0.08)			
Solar radiation	0.10	6.152	0.025	0.70	-	3.6
		(22.24)	(0.11)			
Air pollution	0.10	-5.681	0.011	0.61	+	3.8
		(119.84)	(0.09)			

Notes: The dependent variable in all regressions is the total number of contagions per 100,000 inhabitants from the Italian MCP measured at the provincial level, whereas the regressors are measured at the provincial level. The results reported correspond to the estimation of all the models in the model space including any combination of the 14 variables. We use a fixed BRIC *g*-prior on the parameters and a binomial model prior with prior mean model size equal to 7 in all cases. Variables are ranked by column (1), the posterior inclusion probability. Columns (2) and (3) reflect the conditional posterior mean and the standardized conditional posterior mean for the linear marginal effects of each variable, respectively. Column (4) is the sign certainty probability, a measure of our posterior confidence in the sign of the coefficient. Column (5) shows the expected effect in line with the analysis of the potential determinants in Section (4). Column (6) reports the averaged share of the model's R^2 attributed to each variable when calculating the LMG, CAR, GEN, and PMVD relative importance metrics decompositions. Standard deviations in parentheses. * Significant at 10% level, ** significant at 5% level, *** significant at 1% level.

(18.5%). Finally, we find the effect of provincial temperatures on the provincial COVID-19 incidence is negative in 100% of models (of -0.204 standard deviations) and that it is statistically significant at the 1% level, as it occurs at the regional level. Taken together, the results between temperature and COVID-19 severity seem

weaker at the provincial level. Nonetheless, our main finding of temperature being a top factor hindering the spread of the epidemic remains unaltered.

Finally, we would like to discuss the changes in the role of some variables when running this robustness check. We find differences regarding the statistical significance of testing and population density. We attribute these differences to the fact that the grouping criterion in the aggregation from NUTS-3 to NUTS-2 affects the relative between and within regional variability of the two samples, decreasing the estimation efficiency and ultimately signaling that a potential MAUP is somehow 'contaminating' our baseline analysis (see Arbia & Petrarca, 2011). However, the most remarkable difference between the results obtained using the NUTS-2 level and NUTS-3 level samples is that, at the NUTS-3 level, social mobility seems to be far more relevant. This is because it displays higher PIPs, a higher share of the R^2, and a statistically significant positive effect. As said before, a potential explanation is that the aggregation of provincial mobility at the NUTS-2 level distorts the true relationship between mobility and infections. This could occur because of a region can hide a high degree of heterogeneity in subregional mobility patterns that are heterogeneous and, arguably, have heterogeneous effects on the spread of the virus. Another explanation for the stronger observed effects of mobility at the provincial level is that mobility, at this level of aggregation, mainly captures relatively short distances of travel and might be fed by individuals with closer and more direct social contacts among themselves, thereby increasing the probability of infection relative to social interactions based on longer-distance mobility.

6.2.4 | Time window, spillovers, and measurement errors

Another concern is that the main results might not be robust to the window of time considered and the role played by spatial spillovers. We now check if the results hold when considering these issues.

To investigate if the results are dependent on the time window, we now carry out a period-by-period BMA analysis. Thus, for each time $t = 1,\ldots,T$, we run:

$$y_i(t) = \alpha + \sum_{h=1}^{K} \beta_h X_{ih} + u_i(t) \tag{11}$$

where $y_i(t)$ is the number of cumulative cases in region i at period t. These period-by-period regressions are able to capture any functional form for the path of the number of cumulative cases over time for each X_h, while the computation of PIPs at each date helps us to identify the time variability of variable importance from a Bayesian perspective.

A feature of the data on infections and temperatures in Italy already highlighted in Section 3 is that there are geographical clusters of regions with high incidence and there exists positive and significant positive spatial dependence (Benedetti et al., 2020; Ghosh & Cartone, 2020). To account for this spatial correlation, we also consider a modified version of Equation 11 and introduce a spatial lag term Wy, as in Andersen et al. (2020) and Ghosh and Cartone (2020), which allows us to capture global spillover/neighboring effects. Hence, this specification captures the possibility of contagions in any region i, y_i to be affected by the incidence in the rest of the system of interacting regions $-i$. This seems plausible given that the mobility of infected individuals between regions may have contributed to the spread of the disease across borders before the lockdown took place, and omitting this term could bias the estimated impact of temperature. The period-by-period spatial lag model (SLM) regressions are given by:

$$y_i(t) = \alpha + \rho \sum_{j=1}^{N} W_{ij} y_j(t) + \sum_{h=1}^{K} \beta_h X_{ih} + u_i(t) \tag{12}$$

where ρ captures the spillover effect, and W is a $N \times N$ matrix with elements w_{ij} that describe the spatial influence of each pair of regions i and j. In the empirical analysis, we specify W as a 5-nearest neighbors. To produce PIPs in the SLM, we rely on a Bayesian two-stage least squares procedure such that, for each date, we instrument $W_{ij}y_j(t)$ with the spatial lag of X, following Kelejian et al. (2013). In the spatial BMA analysis, we use a partial derivative interpretation of the impact from changes to the variables to provide evidence on the effect of temperature (i.e., we calculate $\frac{dy}{dX_h} = (I_n - \rho W)^{-1}\beta_h$) and report the average direct, indirect, and total effects across sample units following LeSage and Pace (2009)).[7]

An important issue in these specifications is to avoid linking the mean temperature of a future period $t + h$ to actual contagions in t (Palialol et al., 2020). Thus, we need to account for delays between the time from infection and the record date of the tests, which in Italy was around 17 days.[8] Because our measurement of mean temperature includes temperatures of February 29, our period-by-period analysis begins March 17 and goes up to May 15, covering the first wave and the end of restrictions.

A final concern is that measurement errors are likely to be present in our key dependent variable given that a large share of cases may have not been detected and these measurement errors may not be the same across regions. To address this issue, we estimate the percentage of symptomatic COVID-19 cases reported using case fatality ratio estimates, correcting for delays between confirmation and death following Nishiura et al. (2009) and Russell et al. (2020). Figure A4 shows the result of correcting the official data of infections taking into account regional differences in the under-reporting of cases, which range from the 77.1% of Basilicata (ITF5) to the 94.8% of Lombardy (ITC4), whereas Table (A2) provides the corrected figures in each case for the interested reader. An implication of the results of this data correction procedure is that both the total and relative epidemic size of each region differs substantially from the official data. Specifically, for our baseline date, on April 15, we estimate that there were more than 2.387 millions cases, which is 14 times higher than the 0.168 million tested positive and reported by the official data of the CPM.

To summarize our checks, we have four different model specifications. There are two outcomes: the total cases and the total cases after correcting for under-reporting. There are two econometric specifications: a nonspatial and a spatial lag model. Thus, we estimate the 16,384 candidate models based on alternative combinations of regressors for each of the model specifications for 60 different windows of time. The main results of these sensitivity checks are shown in Figures 3,4 and 5. [9]

As observed in Figures 3 and 4, even if there is significant time variation across specifications and within specifications, the estimated posterior mean effect of temperature is always negative irrespective of the spatial/nonspatial configuration and irrespective of the use of official data or data corrected for under-reporting. In general, we find the direct effects and total effects of temperature to be statistically significant at the 5% level, whereas the indirect effects are not significant in many of the windows considered. This can be attributed to the fact that the lockdown may have decreased cross-regional diffusion, such that a change in temperature in regions $-i$ after some point became irrelevant for infections in i. As observed in Figures 3 and 4, the omission of the spatial lag term in the nonspatial specification produces an underestimation of the marginal effect of temperature in the two datasets, as the total effects are much larger than the point estimate of the nonspatial model. Overall, these figures suggest that the negative link between temperature and infection holds when accounting for spatial interactions in COVID-19 incidence across regions.

[7]In this type of spatial model, a change in a specific regressor in region i exerts a *direct effect* on the dependent variable in that region, but also an *indirect effect* on the remaining regions. In our setting, the direct effect captures the average change in the infections in a particular region caused by a one-unit change in that region's regressor X_h. In turn, the indirect effect reflects the aggregate impact on infections in a specific region caused by the change in a regressor in neighboring regions. The *total effect* is the sum of the direct and indirect effects.

[8]5.2 days (4.1-7.0) of incubation period implying the 95th percentile of the distribution at 12.5 days and 3.6 additional days of test delays.

[9]In Table A3 in the Appendix, we provide a comparison of the point estimates of the BMA and spatial BMA with official and corrected cumulative incidence data by April 15. In Table A4, we show the model-averaged direct, indirect, and total effects of the *spatial lag* model. Finally, in Table A5 in the Appendix, we provide further robustness checks on the role played by temperature when employing different definitions of the spatial weights matrix W.

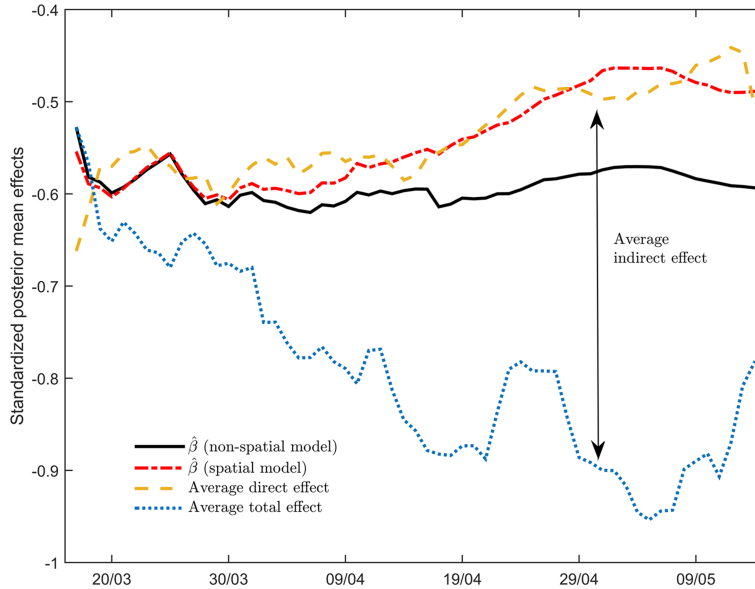

FIGURE 3 The effect of temperature over time: official data

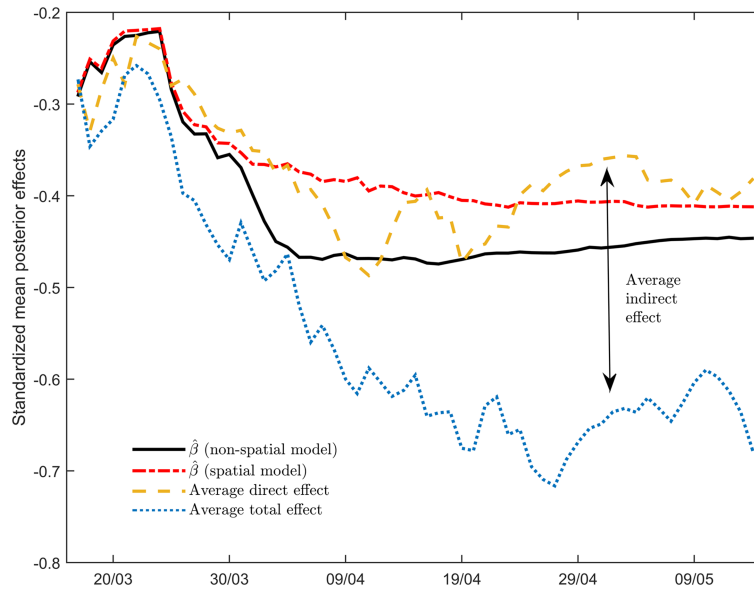

FIGURE 4 The effect of temperature over time: corrected data

Similarly, we find that the time pattern of the PIPs of temperature is above 50% for most of the time sample considered, irrespective of the setup employed. In fact, in Figure 5 we can observe that, when we use the dataset that corrects the figures for the under-reporting of cases, in both the spatial lag model and in the nonspatial one, the PIPs of temperature are only below the 50% threshold the last days of March whereas from April 1 to May 15 they

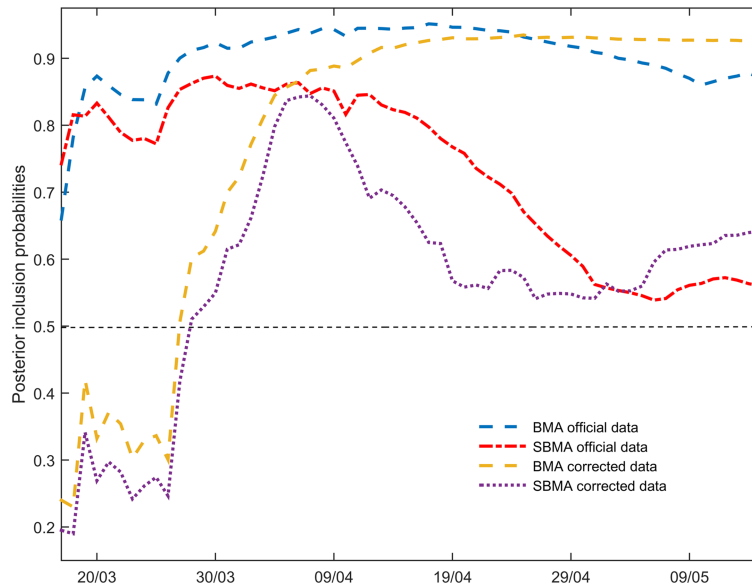

FIGURE 5 The importance of temperature over time

increase substantially to the 67% and 95% marks, respectively.[10] On the other hand, when we use the official data, PIPs are always above 50% in all periods.

6.2.5 | Unobserved heterogeneity

The specifications employed so far include different controls based on a review of the literature. However, one may still argue that the effect of temperature on the dependent variable could simply be capturing the effect of some omitted (potentially spatially correlated) determinant of infections. Therefore, to examine this issue in greater detail, we now estimate a dynamic spatial panel data model with regional fixed and time-period fixed effects using daily data of temperatures and infections. This setup has the advantage of allowing us to control for all time-invariant factors affecting regional infections (i.e., the spatial distribution of the Chinese population).

Specifically, and for the purpose of comparison, we have estimated the following two dynamic panel specifications (nonspatial and spatial) for the period ranging from February 24 to May 15 of 2020:

$$\Delta y_t = \mu + \iota_n \alpha_t + \tau \Delta y_{t-1} + Temp_{t-l}\beta + \epsilon_t \tag{13}$$

$$\Delta y_t = \mu + \iota_n \alpha_t + \tau \Delta y_{t-1} + \rho W \Delta y_t + \eta W \Delta y_{t-1} + Temp_{t-l}\beta + \epsilon_t \tag{14}$$

where Δy_t is a $N \times 1$ vector consisting of observations for the new daily cases for every region $i = 1,\ldots,N$ at a particular point in time $t = 1,\ldots,T$ provided by the MCP, μ and α_t refer to spatial and time-period fixed effects, the terms $\Delta y_t - 1, W\Delta y_t$, and $W\Delta y_t - 1$ denote the time, spatial and space–time lag, respectively, and $Temp_{t-l}$ is the lth period lagged value of temperatures (we present here the results for the value for $l = 17$ days). The spatial weights matrix

[10]One explanation for the lower PIPs of the average temperatures when using the corrected series of infections during March is that the accuracy of the estimate of the true epidemic size estimate is lower on those dates than during April and May of 2020. The reason is that the reliability of the correction procedure implemented following Russell et al. (2020) increases with the number of cases and the length of the time series.

W is again a 5-nearest neighbor specification. We use a first differences specification because the model when using the level series of infections per 100,000 inhabitants (y_t) did not satisfy the stability condition of $\tau + \rho + \eta < 1$ (see Yu et al., 2012). As shown in Tables 7 and 8, the negative impact of temperature on infections for both the regional level and the provincial level samples are statistically significant, giving us confidence in the strength of our cross-sectional findings.

Taken together, the results of all these sensitivity checks suggest temperature is a key factor to understanding regional epidemic disparities in Italy during the first wave of the COVID-19 pandemic.

TABLE 7 Panel data estimates

	Provincial level sample		Regional level sample	
	Nonspatial	Spatial	Nonspatial	Spatial
$\Delta Y(t-1)$	0.229***	0.189***	0.481***	0.428***
	(21.99)	(16.40)	(22.74)	(18.78)
Temperature	-0.577***	-0.130***	-0.460***	-0.077***
	(-7.63)	(-5.32)	(-5.087)	(-2.608)
$W * \Delta Y(t-1)$		0.142***		0.349***
		(8.36)		(8.62)
$W * \Delta Y(t)$		0.469***		0.152***
		(34.04)		(4.191)
R^2	0.456	0.494	0.681	0.689
Log-like	-2772,4	-2771,5	-45103	-45074

Notes: The dependent variable in all regressions is the total number of contagions per 100,000 inhabitants provided by the Italian MCP. To estimate the dynamic spatial panel model, we use the bias-corrected quasi maximum likelihood (BCQML) estimator of Lee and Yu (2010) for dynamic spatial panels and a 5-nearest neighbors row-normalized W matrix. *** significant at 1% level, t-statistics in parentheses.

TABLE 8 Direct, indirect, and total effects

	Direct Effects	Indirect Effects	Total Effects
	Provincial level sample		
Temperature	-0.1376***	-0.1095***	-0.247***
	(-5.03)	(-4.99)	(-5.06)
	Regional level sample		
	Direct	Indirect	Total
	Effects	Effects	Effects
Temperature	-0.0771***	-0.0133***	-0.0905***
	(-2.31)	(-2.030)	(-2.32)

Notes: The dependent variable in all regressions is the total number of contagions per 100,000 inhabitants provided by the Italian MCP. Inferences regarding the statistical significance of these effects are based on the variation of 1,000 simulated parameter combinations drawn from the variance–covariance matrix implied by the BCQML estimates. *** Significant at 1% level, t-statistics in parentheses.

7 | CONCLUSIONS

This study has examined the relationship between temperature and COVID-19 severity differentials in a sample of Italian regions during the period covering the 'first wave' of the pandemic. The key contribution of this analysis is methodological given that we consider the effect of a greater number of determinants than previous studies and we employ BMA techniques to account for model uncertainty and rank the factors in terms of importance.

We compute the PIPs for the different indicators to generate a probabilistic ranking of relevance for the various contagion determinants. The analysis reveals that temperature is a key determinant shaping regional reactions to the epidemic outbreak in Italy, with an inclusion probability of 92% at the regional level. We find that the observed negative and statistically significant effect on viral transmission is robust to a variety of model specifications, with the most plausible explanation for this relationship being the fact that lower outdoor temperatures may have increased the efficiency of viral propagation, decreasing host defenses, and favored indoor social interactions, which without protective equipment may have fueled massive airborne transmission in closed spaces. Sensitivity checks reveal that the negative link between temperature and COVID-19 severity is robust to different modeling settings. Furthermore, the computation of relative importance metrics that allow us to perform an accurate partitioning of the model's fit to the data also confirms this result as temperature explains 30% of the observed differentials.

Among all the robustness checks performed, the one that seems to have the strongest effects is that of the scale of analysis. On provincial level analysis, the distance to the epicenter or the degree of mobility appear to have a higher importance than temperature. In this context, temperature obtains a PIP of 75% and explains 13.5% of the R^2, which suggests that the link is weaker at this level of resolution. Nevertheless, provincial temperature is ranked in third place among all of our explanatory factors and displays a statistically significant negative impact.

Although the limited spatial coverage of the analysis implies that our main findings should be taken with caution and cannot be extrapolated elsewhere, the results of the paper raise potentially important policy implications, especially at a time in which there is an active public debate on the most appropriate instruments to reduce the impact of the epidemic. Because of the strong importance that our modeling exercise attributes to temperature, delays in lockdown policies, and mobility, we interpret our results as indicative that, in the absence of herd immunity, the relaxation of lockdown measures or mobility restrictions combined with a drop in temperature may pose major problems to controlling the pandemic. To deal with the challenge posed by the epidemic, scaling-up of vaccination, active surveillance on emerging variants, and fast quarantine/lockdown responses by health authorities will be needed during the years 2021 and 2022. In addition, as there is overwhelming evidence that inhalation of SARS-CoV-2 represents a major transmission route and that in closed spaces aerosols containing infectious virus can accumulate effectively, health authorities of regions with warmer climate should encourage to move economic and education activities outdoors whenever possible. In colder regions, protective measures focusing on ventilation and air quality control could be an alternative option to increase resilience against the pandemic.

ACKNOWLEDGMENTS

The authors gratefully acknowledge the managing editor and two anonymous referees for their numerous insightful comments and constructive suggestions that have helped to significantly improve the work. The research has received financial support from the Spanish Ministry of Economy and Competitiveness (Project ECO2016-76681-R).

ORCID

Vicente Rios https://orcid.org/0000-0002-9678-1379

REFERENCES

Ahmadi, M., Sharifi, A., Dorosti, S., Ghoushchi, S. J., & Ghanbari, N. (2020). Investigation of effective climatology parameters on COVID-19 outbreak in Iran. *Science of the Total Environment*, *729*, 138705.

Alvarez, F. E., Argente, D. & Lippi, F. (2020). A simple planning problem for COVID-19 lockdown. (w26981): National Bureau of Economic Research.

Andersen, L., Harden, S., Sugg, M., Runkle, J., & Lundquist, T. (2020). Analyzing the spatial determinants of local COVID-19 transmission in the United States. *Science of the Total Environment*, *754*, 142396.

Arbia, G., & Petrarca, F. (2011). Effects of MAUP on spatial econometric models. *Letters in Spatial and Resource Sciences*, *4*(3), 173–185. https://doi.org/10.1007/s12076-011-0065-9

Arenas, A., Cota, W., Gómez-Gardeñes, J., Gómez, S., Granell, C., Matamalas, J. T., Soriano-Paños, D., & Steinegger, B. (2020). Modeling the Spatiotemporal Epidemic Spreading of COVID-19 and the Impact of Mobility and Social Distancing Interventions. *Physical Review X*, *10*(4), 041055.

Auler, A. C., Cássaro, F. A. M., da Silva, V. O., & Pires, L. F. (2020). Evidence that high temperatures and intermediate relative humidity might favor the spread of COVID-19 in tropical climate: A case study for the most affected Brazilian cities. *Science of the Total Environment*, *729*, 139090.

Bashir, M. F., Ma, B., Komal, B., Bashir, M. A., Tan, D., & Bashir, M. (2020). Correlation between climate indicators and COVID-19 pandemic in New York, USA. *Science of the Total Environment*, *728*, 138835.

Benedetti, R., Piersimoni, F., Pignataro, G., & Vidoli, F. (2020). Identification of spatially constrained homogeneous clusters of COVID–19 transmission in Italy. *Regional Science Policy & Practice*, *12*(6), 1169–1187.

Bhagat, R. K., Wykes, M. D., Dalziel, S. B., & Linden, P. F. (2020). Effects of ventilation on the indoor spread of COVID-19. *Journal of Fluid Mechanics*, *903*(F1), 1–17.

Briz-Redón, A., & Serrano-Aroca, A. (2020). A spatio-temporal analysis for exploring the effect of temperature on COVID-19 early evolution in Spain. *Science of the Total Environment*, *728*, 138811.

Bukhari, Q., & Jameel, Y. (2020). Will coronavirus pandemic diminish by summer? Available at SSRN 3556998.

Cannell, J. J., Vieth, R., Umhau, J. C., Holick, M. F., Grant, W. B., Madronich, & Giovannucci, E. (2006). Epidemic influenza and vitamin D. *Epidemiology & Infection*, *134*(6), 1129–1140.

Cartení, A., Di Francesco, L., & Martino, M. (2020). How mobility habits influenced the spread of the COVID-19 pandemic: Results from the Italian case study. *Science of the Total Environment*, *741*, 140489.

Chan, K. H., Peiris, J. S., Lam, S. Y., Poon, L. L. M., Yuen, K. Y., & Seto, W. H. (2011). The effects of temperature and relative humidity on the viability of the SARS coronavirus. *Advances in Virology*, *2011*, 1–7.

Chan, K. H., Sridhar, S., Zhang, R. R., Chu, H., Fung, A. F., Chan, & Yuen, K. Y. (2020). Factors affecting stability and infectivity of SARS-CoV-2. *Journal of Hospital Infection*, *106*(2), 226–231.

Charaudeau, S., Pakdaman, K., & Boelle, P. Y. (2014). Commuter mobility and the spread of infectious diseases: Application to influenza in France. *PloS One*, *9*(1), e83002.

Charron, N., Dijkstra, L., & Lapuente, V. (2014). Regional governance matters: Quality of government within European Union member states. *Regional Studies*, *48*(1), 68–90.

Cui, Y., Zhang, Z. F., Froines, J., Zhao, J., Wang, H., Yu, S. Z., & Detels, R. (2003). Air pollution and case fatality of SARS in the People's Republic of China: An ecologic study. *Environmental Health*, *2*(1), 15.

Duan, S. M., Zhao, X. S., Wen, R. F., Huang, J. J., Pi, G. H., Zhang, & Dong, X. P. (2003). Stability of SARS coronavirus in human specimens and environment and its sensitivity to heating and UV irradiation. *Biomedical and Environmental Sciences: BES*, *16*(3), 246–255.

Ezcurra, R., & Rios, V. (2019). Quality of government and regional resilience in the European Union. Evidence from the Great Recession. *Papers in Regional Science*, *98*(3), 1267–1290.

Fang, W., & Wahba, S. (2020). Urban Density Is Not an Enemy in the Coronavirus Fight: Evidence from China. [BlogPost]. Retreived March 30, 2020 from https://blogs.worldbank.org/sustainablecities/urban-density-not-enemy-coronavirus-fight-evidence-china

Feldman, B. (2005). Relative Importance and Value. Manuscript version 1.1, 2005-03-19, URL https://www.prismanalytics.com/docs/RelativeImportance.pdf

Genizi, A. (1993). Decomposition of R2 in multiple regression with correlated regressors. *Statistica Sinica*, *3*, 407–420.

Ghosh, J., & Ghattas, A. E. (2015). Bayesian variable selection under collinearity. *The American Statistician*, *69*(3), 165–173.

Ghosh, P., & Cartone, A. (2020). A Spatio–temporal analysis of COVID–19 outbreak in Italy. *Regional Science Policy & Practice*, *12*(6), 1047–1062.

Gromping, U. (2007). Estimators of relative importance in linear regression based on variance decomposition. *The American Statistician*, *61*(2), 139–147.

International Monetary Found. (2020). World Economic Outlook, April 2020: Chapter 1. World Economic Outlook Reports.

Iqbal, M. M., Abid, I., Hussain, S., Shahzad, N., Waqas, M. S., & Iqbal, M. J. (2020). The effects of regional climatic condition on the spread of COVID-19 at global scale. *Science of the Total Environment*, *739*, 140101.

Johnson, J. W., & LeBreton, J. M. (2004). History and use of relative importance indices in organizational research. *Organizational Research Methods*, *7*(3), 238–257.

Kapitsinis, N. (2020). The underlying factors of the COVID-19 spatially uneven spread. Initial evidence from regions in nine EU countries. *Regional Science Policy & Practice*, *12*(6), 1027–1045.

Kelejian, H. H., Murrell, P., & Shepotylo, O. (2013). Spatial spillovers in the development of institutions. *Journal of Development Economics*, *101*, 297–315.

Kumar, S. (2020). Effect of meteorological parameters on spread of COVID-19 in India and air quality during lockdown. *Science of the Total Environment*, *745*, 141021.

Lee, L. F., & Yu, J. (2010). A spatial dynamic panel data model with both time and individual fixed effects. *Econometric Theory*, *26*(2), 564–597.

LeSage, J., & Pace, R. K. (2009). *Introduction to spatial econometrics*: Chapman and Hall/CRC.

Lin, J., Huang, W., Wen, M., Li, D., Ma, S., Hua, & Zhang, Q. (2020). Containing the spread of coronavirus disease 2019 (COVID-19): Meteorological factors and control strategies. *Science of the Total Environment*, *744*, 140935.

Lowen, A. C., & Steel, J. (2014). Roles of humidity and temperature in shaping influenza seasonality. *Journal of Virology*, *88*(14), 7692–7695.

Ma, Y., Zhao, Y., Liu, J., He, X., Wang, B., Fu S., Yan, J., Niu, J., Zhou, J., & Luo, B. (2020). Effects of temperature variation and humidity on the death of COVID-19 in Wuhan, China. *Science of the Total Environment*, *724*, 138226.

Makinen, T. M., Juvonen, R., Jokelainen, J., Harju, T. H., Peitso, A., Bloigu, & Hassi, J. (2009). Cold temperature and low humidity are associated with increased occurrence of respiratory tract infections. *Respiratory Medicine*, *103*, 456–462.

Martineau, A. R., Jolliffe, D. A., Hooper, R. L., Greenberg, L., Aloia, J. F., Bergman, & Goodall, E. C. (2017). Vitamin D supplementation to prevent acute respiratory tract infections: systematic review and meta-analysis of individual participant data. *BMJ*, *356*, i6583.

Méndez-Arriaga, F. (2020). The temperature and regional climate effects on communitarian COVID-19 contagion in Mexico throughout phase 1. *Science of the Total Environment*, *735*, 139560.

Merow, C., & Urban, M. C. (2020). Seasonality and uncertainty in COVID-19 growth rates. medRxiv.

Miller, S. L., Nazaroff, W. W., Jimenez, J. L., Boerstra, A., Buonanno, G., Dancer, S. J., Kurnitski, J., Marr, L. C., Morawska, L., & Noakes, C. (2020). Transmission of SARS-CoV-2 by inhalation of respiratory aerosol in the Skagit Valley Chorale superspreading event. Indoor Air (forthcoming).

Moral-Benito, E. (2015). Model averaging in economics: An overview. *Journal of Economic Surveys*, *29*(1), 46–75.

Morawska, L., & Cao, J. (2020). Airborne transmission of SARS-CoV-2: The world should face the reality. *Environment International*, *139*, 105730.

Morawska, L., Tang, J. W., Bahnfleth, W., Bluyssen, P. M., Boerstra, A., Buonanno, G., Cao, J., Dancer, S., Floto, A., Franchimon, F., & Haworth, C. (2020). How can airborne transmission of COVID-19 indoors be minimised? *Environment International*, *142*, 105832.

Nishiura, H., Klinkenberg, D., Roberts, M., Nishiura, H., Klinkenberg, D., Roberts, M., & Heesterbeek, J. A. (2009). Early epidemiological assessment of the virulence of emerging infectious diseases: A case study of an influenza pandemic. *PLoS One*, *4*(8), e6852.

Oliveiros, B., Caramelo, L., Ferreira, N. C., & Caramelo, F. (2020). Role of temperature and humidity in the modulation of the doubling time of COVID-19 cases. medRxiv.

Openshaw, S. (1984). Ecological fallacies and the analysis of areal census data. *Environment and Planning A*, *16*(1), 17–31. https://doi.org/10.1068/a160017

Orea and Alvarez (2020). How effective has the Spanish lockdown been to battle COVID-19? A spatial analysis of the coronavirus propagation across provinces. FEDEA Documento de trabajo, *3*, 1-33

Oto-Peralías, D. (2020). Regional correlations of COVID-19 in Spain.

Paez, A., Lopez, F. A., Menezes, T., Cavalcanti, R., & Pitta, M. G. D. R. (2020). A spatio-temporal analysis of the environmental correlates of COVID-19 incidence in Spain. *Geographical Analysis*, *53*(3), 397–421.

Palialol, B., Pereda, P., & Azzoni, C. (2020). Does weather influence COVID-19 transmission? *Regional Science Policy & Practice*, *12*(6), 981–1004.

Pan, J., Yao, Y., Liu, Z., Meng, X., Ji, J. S., Qiu, & Kan, H. (2020). Warmer weather unlikely to reduce the COVID-19 transmission: An ecological study in 202 locations in 8 countries. *Science of the Total Environment*, *753*, 142272.

Pedrosa, R. H. (2020). The dynamics of Covid-19: Weather, demographics and infection timeline. medRxiv.

Perone, G. (2020). The determinants of COVID-19 case fatality rate (CFR) in the Italian regions and provinces: an analysis of environmental, demographic, and healthcare factors. *Science of The Total Environment*, *755*, 142523.

Pluchino, A., Biondo, A. E., Giuffrida, N., Inturri, G., Latora, V., Le Moli, R., Rapisarda, A., Russo, G., & Zappala, C. (2021). A novel methodology for epidemic risk assessment of COVID-19 outbreak. *Scientific Reports*, *11*(1), 1–20.

Prata, D. N., Rodrigues, W., & Bermejo, P. H. (2020). Temperature significantly changes COVID-19 transmission in (sub) tropical cities of Brazil. *Science of the Total Environment*, *729*, 138862.

Qi, H., Xiao, S., Shi, R., Ward, M. P., Chen, Y., Tu, & Zhang, Z. (2020). COVID-19 transmission in Mainland China is associated with temperature and humidity: A time-series analysis. *Science of the Total Environment*, *728*, 138778.

Rios, V., & Gianmoena, L. (2020). The link between quality of government and regional resilience in Europe. *Journal of Policy Modeling*, *42*(5), 1064–1084.

Romer, P. (2020). Even A Bad Test Can Help Guide the Decision to Isolate: Covid Simulations Part 3. [BlogPost]. Retreived from https://paulromer.net/covid-sim-part3/

Russell, T. W., Golding, N., Hellewell, J., Abbott, S., Wright, L., Pearson, & Eggo, R. M. (2020). Reconstructing the early global dynamics of under-ascertained COVID-19 cases and infections. *BMC Medicine*, *18*(1), 1–9.

Sajadi, M. M., Habibzadeh, P., Vintzileos, A., Shokouhi, S., Miralles-Wilhelm, F., & Amoroso, A. (2020). Temperature and latitude analysis to predict potential spread and seasonality for COVID-19. Available at SSRN 3550308.

Shakil, M. H., Munim, Z. H., Tasnia, M., & Sarowar, S. (2020). COVID-19 and the environment: A critical review and research agenda. *Science of the Total Environment*, *745*, 141022.

Steel, M. F. (2020). Model averaging and its use in economics. *Journal of Economic Literature*, *58*(3), 644–719.

Van Doremalen, N., Bushmaker, T., & Morris, D. (2020). Aerosol and surface stability of HCoV-19 (SARS-CoV-2) compared to SARS-CoV-1. medRxiv.

Verity, R., Okell, L. C., Dorigatti, I., Winskill, P., Whittaker, C., Imai, N., Cuomo-Dannenburg, G., Thompson, H., Walker, P. G., Fu, H., & Dighe, A. (2020). Estimates of the severity of coronavirus disease 2019: A model-based analysis. *The Lancet Infectious Diseases*, *20*(6), 669–677.

Wang, C. J., Ng, C. Y., & Brook, R. H. (2020a). Response to COVID-19 in Taiwan: Big data analytics, new technology, and proactive testing. *JAMA*, *323*(14), 1341–1342.

Wang, J., Tang, K., Feng, K., & Lv, W. (2020b). High temperature and high humidity reduce the transmission of COVID-19. Available at SSRN 3551767.

World Health Organization (2005). Using climate to predict infectious disease epidemics.

World Health Organization (2020a). Report of the WHO-China Joint Mission on Coronavirus Disease 2019 (COVID-19).

World Health Organization (2020b). Modes of transmission of virus causing COVID-19: Implications for IPC precaution recommendations. *Scientific Brief*. World Health Organization.

World Health Organization (2020c). Coronavirus disease 2019 (COVID-19) situation report – 32.

Wu, X., Lang, L., Ma, W., Song, T., Kang, M., He, & Ling, L. (2018). Non-linear effects of mean temperature and relative humidity on dengue incidence in Guangzhou, China. *Science of the Total Environment*, *628*, 766–771.

Wu, X., Nethery, R. C., Sabath, B. M., Braun, D., & Dominici, F. (2020). Exposure to air pollution and COVID-19 mortality in the United States. medRxiv.

Xie, J., & Zhu, Y. (2020). Association between ambient temperature and COVID-19 infection in 122 cities from China. *Science of the Total Environment*, *724*, 138201.

Yao, Y., Pan, J., Liu, Z., Meng, X., Wang, W., Kan, H., & Wang, W. (2020). No association of COVID-19 transmission with temperature or UV radiation in Chinese cities. *European Respiratory Journal*, *55*(5), 2000517.

Yongjian, Z., Jingu, X., Fengming, H., & Liqing, C. (2020). Association between short-term exposure to air pollution and COVID-19 infection: Evidence from China. *Science of the Total Environment*, *727*, 138704.

Yu, J., Jong, R., & Lee, F. (2012). Estimation for spatial dynamic panel data with fixed effects: The case of spatial cointegration. *Journal of Econometrics*, *167*, 16–37.

Zeugner, S., & Feldkircher, M. (2015). Bayesian model averaging employing fixed and flexible priors: The BMS package for R. *Journal of Statistical Software*, *68*(4), 1–37.

Zhang, R., Li, Y., Zhang, A. L., Wang, Y., & Molina, M. J. (2020). Identifying airborne transmission as the dominant route for the spread of COVID-19. *Proceedings of the National Academy of Sciences*, *117*(26), 14857–14863.

Zhang, Z., Xue, T., & Jin, X. (2020). Effects of meteorological conditions and air pollution on COVID-19 transmission: Evidence from 219 Chinese cities. *Science of the Total Environment*, *741*, 140244.

Zoran, M. A., Savastru, R. S., Savastru, D. M., & Tautan, M. N. (2020). Assessing the relationship between surface levels of PM2. 5 and PM10 particulate matter impact on COVID-19 in Milan, Italy. *Science of the Total Environment*, *738*, 139825.

Zuber, V., & Strimmer, K. (2010). Variable importance and model selection by decorrelation. https://arxiv.org/abs/1007.5516

Zuber, V., & Strimmer, K. (2011). High-dimensional regression and variable selection using CAR scores. *Statistical Applications in Genetics and Molecular Biology*, *10*(1), 1–27.

How to cite this article: Rios, V., & Gianmoena, L. (2021). On the link between temperature and regional COVID-19 severity: Evidence from Italy. *Regional Science Policy & Practice*, *13*(S1), 109–137. https://doi.org/10.1111/rsp3.12472